ELSEVIER

Experimental Thermal and Fluid Science 23 (2000) 23–33

Experimental Thermal and Fluid Science

www.elsevier.nl/locate/etfs

An experimental study of the unsteady characteristics of the turbulent near wake of a turbine blade

Marina Ubaldi, Pietro Zunino *

Dipartimento di Macchine, Sistemi Energetici e Trasporti, Università di Genova, Via Montallegro 1, I-16145 Genova, Italy

Received 24 January 2000; accepted 24 July 2000

Abstract

The paper reports the results of an experimental investigation of the time-varying characteristics of the flow in the turbulent near wake behind the central blade of a large-scale turbine cascade. The blade wake has been surveyed by means of a two-component laser Doppler velocimeter (LDV) over a close experimental grid extending from the blade trailing edge to six trailing edge diameters downstream. A phase-locked ensemble averaging technique has been applied to the LDV instantaneous data in order to separate coherent contributions due to large-scale organised structures from random contributions due to turbulence. A reference signal generated by a hot-wire probe, located at a fixed position within the flow, is utilised to associate each LDV velocity realisation with the phase of the vortex shedding. The hot-wire signal provides also an univocal time reference suitable for correlating all single-point measurements, allowing to construct sequences of images which show the time evolution of the organised structures embedded in the flow. In the discussion, the mean flow properties, the periodic structure of the unsteady flow and the vortex shedding mechanism are analysed. Similarities and differences between the present results for a turbine blade wake and those for wakes of circular cylinders are highlighted. Normal stresses due to the periodic motion and those due to turbulence fluctuations are resolved separately. Both contributions have the same order of magnitude in the region close to the trailing edge, where the vortices are forming, but the normal stresses associated with the periodic fluctuations decay more rapidly in streamwise direction.

Keywords: Turbine blade wake; Unsteady flow; Coherent structures; Laser doppler velocimeter

1. Introduction

Wakes from turbine blades are unsteady in character because of the presence of large-scale organised structures, known as von Karman vortex streets. Vortex shedding represents an important cause of energy losses, blade dynamic loadings, mechanical vibrations and noise.

In spite of the importance of this phenomenon, the flow in the wake behind turbine blades is generally viewed as the superposition on a time-averaged flow of an unresolved unsteadiness comprehensive of all the fluctuations regardless of their scale. Only few examples of detailed studies concerning the time-varying characteristics of blade wakes [1] are available in the technical literature, because of the experimental difficulties associated with the large gas velocities and the small blade trailing edge dimension, resulting in very large shedding frequencies and scarce spatial resolution of the measurement. Therefore, our present knowledge on the mechanism of vortex shedding from blade trailing edges is still mainly based on the results of detailed experimental investigations behind cylinders (e.g., [2,3]).

The present contribution is part of a research activity carried out within the framework of a Brite Euram project and aimed at the improvement of the knowledge on the time-varying turbine wake characteristics. The program included systematic investigations on large-scale models carried out in different laboratories making use of complementary experimental techniques. Results concerning the effect of vortex shedding on the unsteady pressure distribution around the blade trailing edge and the details of the unsteady flow in the base region have been previously published [4,5]. The present paper concerns a LDV systematic

* Corresponding author. Tel.: +39-010-353-2448; fax: +39-010-353-2566.

E-mail address: zunmp@unige.it (P. Zunino).

0894-1777/00/$ - see front matter
PII: S0894-1777(00)00030-3

Nomenclature

c	blade chord (m)
D	trailing edge diameter (m)
f	vortex shedding frequency (Hz)
H_{12}	boundary layer shape factor, dimensionless
M_{2is}	Mach number based on outlet isoentropic conditions, dimensionless
n	normal distance from the blade surface (m)
Re_c	Reynolds number based on blade chord and ascade outlet velocity $Re_c = \rho c U_2/\mu$, dimensionless
Re_D	Reynolds number based on trailing edge thickness and cascade outlet velocity $Re_D = \rho D\ U_2/\mu$, dimensionless
Re_θ	Reynolds number based on the boundary layer momentum thickness and free-stream velocity $Re_\theta = \rho\ u_e\theta/\mu$, dimensionless
s	streamwise coordinate along the blade surface (m)
St	Strouhal number $St = fD/U_2$, dimensionless
t	time (s)
T	period of one vortex shedding cycle (s)
u, v	boundary layer velocity components in streamwise and cross-stream directions (m/s)
u', v'	boundary layer velocity fluctuations in streamwise and cross-stream directions (m/s)
U	velocity (m/s)
x	streamwise direction at the cascade outlet (m)
y	cross-stream direction at the cascade outlet (m)

Greeks

δ^*	boundary layer displacement thickness (m)
θ	boundary layer momentum thickness (m)
μ	dynamic viscosity (kg/m s)
ρ	fluid density (kg/m^3)
ω	vorticity (s^{-1})

Subscripts

e	free-stream value
s	in the streamwise direction
n	in the cross-stream direction
1	at the cascade inlet
2	at the cascade outlet

Superscripts and overbars

‘	fluctuating component
—	time averaged
∼	ensemble average

investigation in the turbulent near wake of a turbine blade in cascade. A phase-locked ensemble average technique suitable for LDV measurements has been developed and used together with the triple decomposition scheme for the instantaneous velocity in order to identify the periodic organised structures embedded in the turbulent wake flow.

A key point to the present investigation is the high spatial resolution obtained, thanks to the adoption of a large-scale three-blade cascade, a probe volume of small dimensions and a high precision probe traversing system. Tests were run at a Reynolds number ($Re_c = 1.6 \times 10^6$), which is representative of gas turbine high pressure stages. The resulting test outlet Mach number ($M_{2is} = 0.24$) is low compared with the modern gas turbine Mach number range which extends in the medium–high subsonic and transonic regimes. The present results still can be considered representative for subsonic gas turbines, because, according to the review paper of Cicatelli and Sieverding [1], the vortex shedding Strouhal number in the subsonic regime depends mainly on the boundary layer state at the trailing edge, which is strongly influenced by the Reynolds number, the free-stream turbulence and the streamwise velocity gradients, rather than by the compressibility effects associated with the Mach number variations. In the transonic regime, on the contrary, the shedding mechanism is strongly modified by the formation of the trailing edge shock system [1,6]. The result is an increase of the Strouhal number and the breakdown of the stable von Karman vortex street with the occurrence of highly transient vortex shedding patterns.

2. Experimental details

2.1. Test facility and instrumentation

The experiment was conducted in the DIMSET low speed wind tunnel. The facility is a blow-down continuously operating variable speed tunnel with an open test section of 500×300 mm^2.

The flow was surveyed downstream of the central blade of a three-blade large-scale turbine linear cascade. The blade profile, designed at VKI [4], is representative of a coolable hp gas turbine nozzle blade. A three-blade configuration has been selected in order to have larger blade dimensions within the given test section with the purpose of lowering the vortex shedding frequency and increasing the spatial resolution of the measurements. A schematic of linear cascade and experimental traverses is shown in Fig. 1. The main geometrical parameters of the cascade and the test conditions are summarised in Table 1. The coordinates of the blade are given in [4].

The three blades are instrumented at mid-span with a total of 110 pressure tappings. Periodicity condition was monitored by comparing the pressure distributions on the central blade and the two adjacent ones and achieved by modifying the curvature of the adjustable tailboards and throttling two lateral apertures at the cascade inlet [5].

In the present experiment, a four-beam two-colour laser Doppler velocimeter (LDV) with back-scatter collection optics (Dantec Fiber Flow) has been used. The light source is a 300 mW argon ion laser tuned to 488 nm (blue) and 514.5 nm (green).

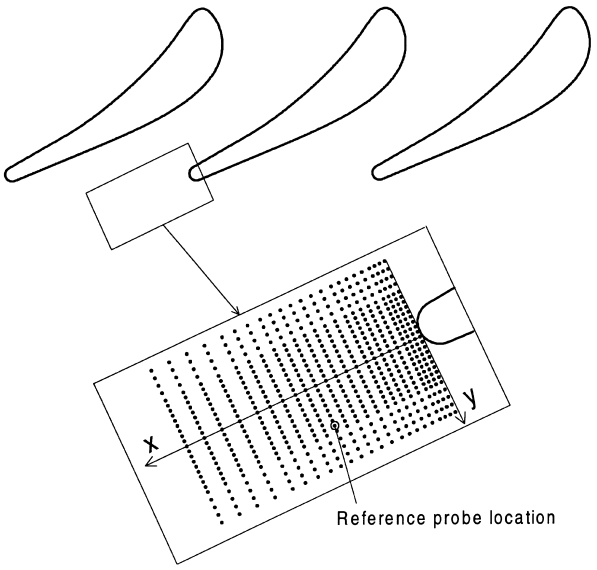

Fig. 1. Schematic of turbine blade cascade and measuring traverses.

Table 1
Cascade geometry and test conditions

Cascade geometry	
Chord length	$c = 300$ mm
Pitch-to-chord ratio	$g/c = 0.7$
Aspect ratio	$h/c = 1.0$
Inlet blade angle	$\beta'_1 = 0°$
Gauging angle	$\beta'_2 = 19.1°$
Test conditions	
Relative inlet total pressure	$p_{t1} = 3060$ Pa
Inlet total temperature	$T_{t1} = 293$ K
Inlet turbulence intensity	$Tu = 1\%$
Outlet isoentropic Mach number	$M_{2is} = 0.24$
Outlet Reynolds number	$Re_c = 1.6 \times 10^6$

The probe consists of an optical transducer head of 60 mm diameter connected to the emitting optics and to the photomultipliers by means of optic fibres. With a front lens of 400 mm focal length and a beam separation of 38 mm, the optical probe volume is 0.12 mm of diameter and 2.4 mm of length. The probe volume was oriented with the larger dimension along the spanwise direction, in order to have better spatial resolution in the blade-to-blade plane. A Bragg cell is used to apply a frequency shift (40 MHz) to one of each pair of beams, allowing to solve directional ambiguity and to reduce angle bias. The signals from the photomultipliers were processed by two burst spectrum analysers (BSA).

The flow was seeded with a 0.5–2 μm atomised spray of mineral oil injected in the flow at about 2 chord upstream of the cascade leading edge.

The probe was traversed using a three-axis computer controlled probe traversing system with a minimum linear translation step of 8 μm.

2.2. Measuring procedure

According to the triple decomposition scheme proposed by Reynolds and Hussain [7] for the study of coherent structures in shear flows, a generic velocity component v in a generic position P can be represented as the sum of the time-averaged contribution $\bar{v}$, the fluctuating component due to the periodic motion $(\tilde{v} - \bar{v})$ and the random fluctuation v'

$$v = \bar{v} + (\tilde{v} - \bar{v}) + v'. \tag{1}$$

The time-varying mean velocity component $\tilde{v}$ can be obtained by ensemble averaging the samples.

$$\tilde{v}(i) = \frac{1}{K_i}\sum_{k=1}^{K_i} v(i,k), \tag{2}$$

where $i = 1, \ldots, I$ is the index of the phases into which a vortex shedding period is subdivided and $k = 1, \ldots, K_i$ is the index of the samples for each window associated with a particular phase i.

The time-averaged velocity component $\bar{v}$ can be simply determined as

$$\bar{v} = \frac{1}{I}\sum_{i=1}^{I} \tilde{v}(i). \tag{3}$$

Ensemble averaged variances, which are proportional to the Reynolds stress normal components, are obtained as

$$\widetilde{v'^2}(i) = \sqrt{\frac{1}{(K_i - 1)}\sum_{k=1}^{K_i}[v(i,k) - \tilde{v}(i)]^2}. \tag{4}$$

In the present experiment, an ensemble averaging technique suitable for LDV data processing has been implemented. The technique makes use of a single-sensor hot-wire probe which is sensitive to the passage of the organised structures in order to generate a reference signal. The hot-wire output is band-pass filtered, amplified and processed by means of an electronic device capable of producing a suitable TTL signal of 5 μs duration in correspondence of the maximum of the hot-wire signal. This phase information is provided to the synchronisation input port of the BSA processors operating in "encoder enabled mode". The arrival time of each LDV velocity realisation is recorded together with the phase reference signal.

To allow the ensemble average, the data are sorted into 50 phase bins each representing a particular phase of the vortex shedding cycle. To obtain statistically accurate ensemble averages of the LDV velocities, 50,000 validated data for each component have been sampled at each measuring point. For a vortex shedding frequency of about 1300 Hz the bin width is 15 μs and the mean number of samples for each bin is 1000.

2.3. Measurement accuracy

A comprehensive review of errors in LDV measurements and guidelines to evaluate them are given by

Boutier [8] and, in the case of turbomachinery applications, by Strazisar [9]. A specific evaluation of the errors for frequency domain processors is given by Modarress et al. [10].

The error on the instantaneous velocity due to random noise from the photomultiplier tube depends on the background scattered light and on the processing technique. BSA can measure with a signal to noise ratio as low as −5 dB, without apparent increase of the S.D. [10]. The resolution of the BSA processor depends on the record length of the FFT and on the background noise. For the present experiment, even in the worst cases, it was below 1% of the mean velocity.

A statistical bias can occur because the arrival times of the measurable particles are not statistically independent on the flow velocity which brings them into the probe volume. If the velocity is not constant in time, the resulting non-uniform data sampling causes an error when simple arithmetic averages are performed. The magnitude of the bias is of the order of the square of the turbulence intensity based on the local mean velocity. The ensemble averaging procedure that has been adopted in the present experiment, where the samples in each bin are statistically independent because they were collected during different cycles, avoids statistical bias, as observed by Lyn et al. [3].

Angle bias occurs when the particle trajectories are not normal to fringe orientation. Moving the fringe pattern in the probe volume by means of the Bragg cell allows to minimise this error. For the present experiment, the angle bias was kept lower than 1% of the mean velocity.

Statistical uncertainty in mean and rms velocities depends on the number of sampled data, turbulence intensity and confidence level [8]. For the present experiment, considering a typical value of 1000 sampled data, a confidence level of 95% and a local turbulence intensity of 30%, uncertainties of ±2% and ±5% are expected for the mean and rms velocities, respectively.

3. Results and discussion

The time-varying characteristics of the blade wake flow is strongly influenced by the boundary layer state at the blade trailing edge [11]. The blade boundary layer development mainly depends on the surface velocity distribution, the Reynolds number and the free-stream turbulence.

In the present experiment, the mid-span surface velocity distribution along the turbine blade is typical of a front-loaded profile with a moderate suction side diffusion rate [12]. The chord based Reynolds number is representative of high pressure stages of gas turbines. Boundary layer measurements along the blade profile, described in details in [12], show that, in case of natural development, the boundary layer at the trailing edge is turbulent on the suction side and laminar-transitional on the pressure side. The mixed boundary layer condition at the trailing edge increases the Strouhal number and results in a broader vortex shedding frequency spectrum [11]. The necessity to have well-defined and reproducible boundary layer conditions at the trailing edge has led to the decision to enforce turbulent conditions also on the pressure side by installing a 0.4 mm diameter trip wire. Due to the large turbulence intensity of turbomachinery flows, the condition of turbulent boundary layer at the blade trailing edge on both pressure and suction sides is expected to be the most representative of real flow conditions.

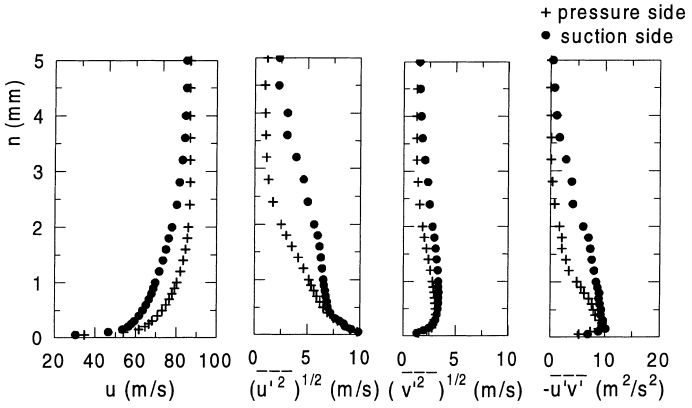

	Suction Side	Pressure Side
s/s_{max}	0.95	0.94
H_{12}	1.36	1.43
δ* (mm)	0.57	0.28
Re_ϑ	2373	1136

Fig. 2. Boundary layer velocity, turbulence profiles and integral parameters at the blade trailing edge.

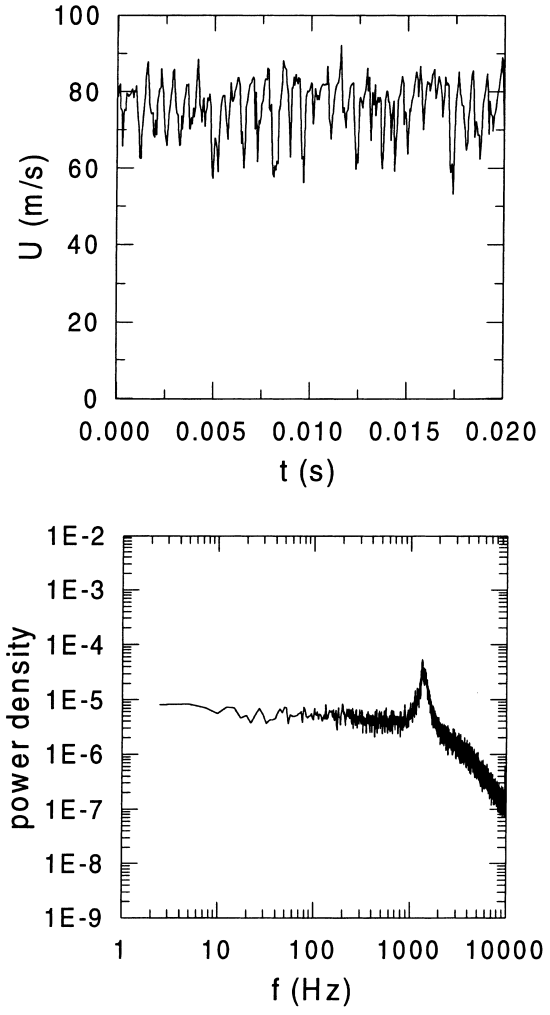

Fig. 3. Instantaneous velocity and power density spectrum of the unsteady flow in the wake: $x/D = 2.0,\ y/D = -1.0$.

Boundary layer velocity and turbulent profiles measured just upstream of the trailing edge are shown in Fig. 2. In the same figure, the integral parameters of the boundary layers are also summarised. Profiles are typical of turbulent boundary layers, but on the suction side the boundary layer thickness is approximately twice that on the pressure side.

In order to get a preliminary overview of the time-varying characteristics of the flow, instantaneous velocities were measured in selected points in the wake by means of a single-sensor hot-wire probe [5]. Time traces and power density spectra of the velocity measured at $x/D = 2.0$ and $y/D = -1.0$ are given in Fig. 3. Details of these measurements and data processing are given in [13]. The flow in the wake is highly unsteady because of both turbulent and organised fluctuations. A peak of energy corresponding to the vortex shedding frequency, can be easily detected at about 1300 Hz. The corresponding Strouhal number $St = f D/U_2$ is 0.26, in close agreement with the value measured at VKI on a cascade with the same blade profile and very similar flow conditions [4].

The systematic investigation of the near wake flow has been performed measuring the velocity components at the nodes of a close experimental grid made of 23 cross-stream traverses ranging from $x/D = 0.0625$ to $x/D = 5.625$. Each traverse consisted of 27 points ranging from $y/D = -1.875$ to $y/D = 1.875$. The origin of the coordinate system is the extremity of the blade trailing edge. The experimental grid is shown in Fig. 1.

3.1. Mean flow properties

Before analysing the periodic structure of the unsteady flow in the wake, a survey of the mean flow field (Fig. 4) can be appropriate, as it is an important term of comparison with numerical predictions and represents

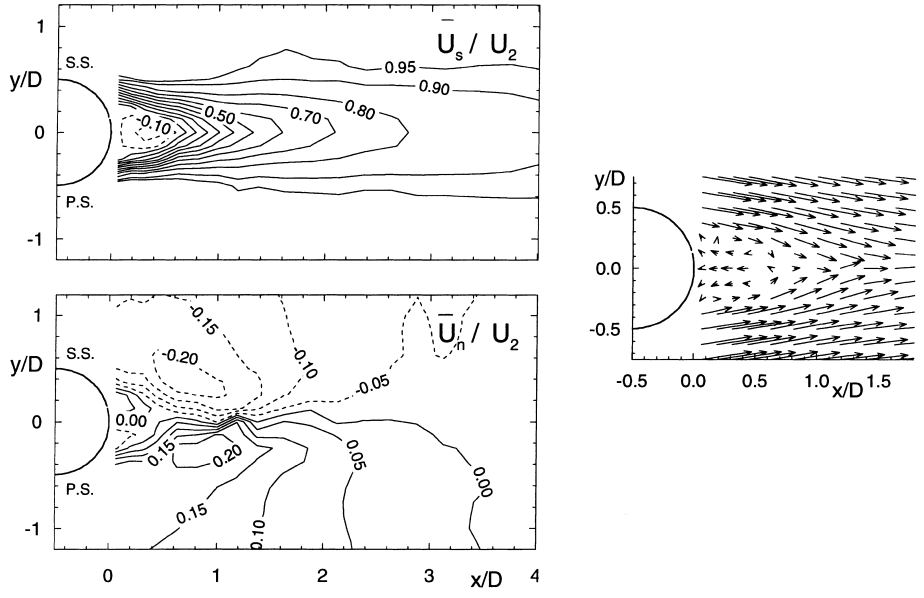

Fig. 4. Time-averaged flow field.

the base flow upon which the motion of organised structures is superimposed.

Streamwise velocity distribution $\bar{U}_s/U_2$ shows the extension and the rapid decay of the wake velocity defect. Because of the continuity condition, large transverse mean velocity components $\bar{U}_n/U_2$ of opposite sign are present on the two sides of the wake. This effect extends in cross-stream direction well beyond the wake defect region and free-stream flow is drawn towards the wake centre.

Both streamwise velocity distribution and vector plot show the extension of the mean separated flow. The mean closure point is about 0.7 D. For circular cylinders this quantity is sensitive to the Reynolds number based on diameter and free-stream velocity Re_D. Cantwell and Coles [2] estimated $x/D = 1$ for $Re_D = 140,000$, Mc Killop and Durst [14] $x/D = 1.65$ for $Re_D = 15,000$. Both experiments were performed in the so-called "shear layer transition regime" [15], characterised by laminar separation from the surface and turbulent transition in the shear layer. In the present investigation, the Re_D value ($Re_D = 85,000$) is intermediate. In spite of that, the boundary layer state at the trailing edge is turbulent on both sides, because of the large-blade chord Reynolds number ($Re_c = 1.6 \times 10^6$), the moderate suction side rearward deceleration and the presence of the trip wire on the pressure side. Boundary layer conditions at the separation points explain the reduced length of the mean recirculating region found in the present investigation as well as the large value of the Strouhal number ($St = 0.26$) which is characteristic of the so called "boundary layer transition or supercritical regime" of circular cylinders with $Re_D > 10^6$ [16].

3.2. Ensemble averaged velocity components

Figs. 5–7 show the temporal sequence of the periodic characteristics of the wake flow for four instants in a vortex shedding period ($t/T = 0, 0.25, 0.50, 0.75$).

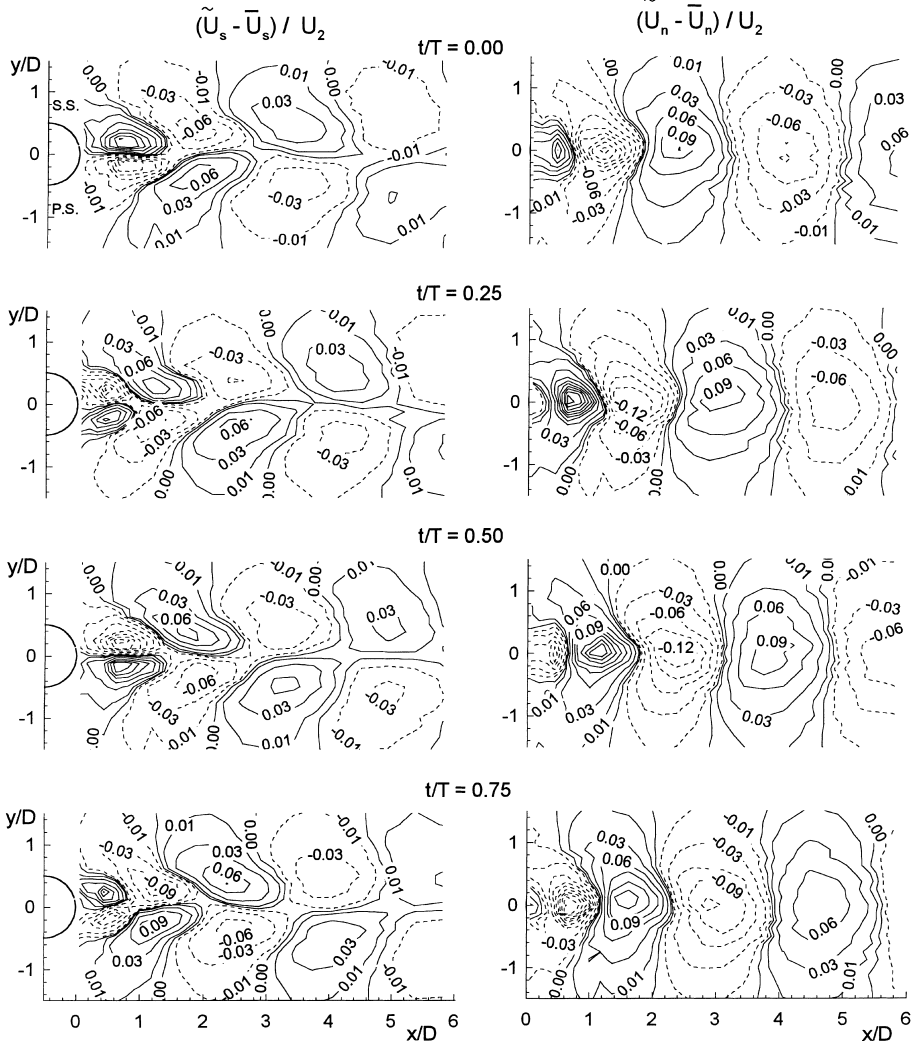

Fig. 5. Contours of the periodic velocity components at successive phases.

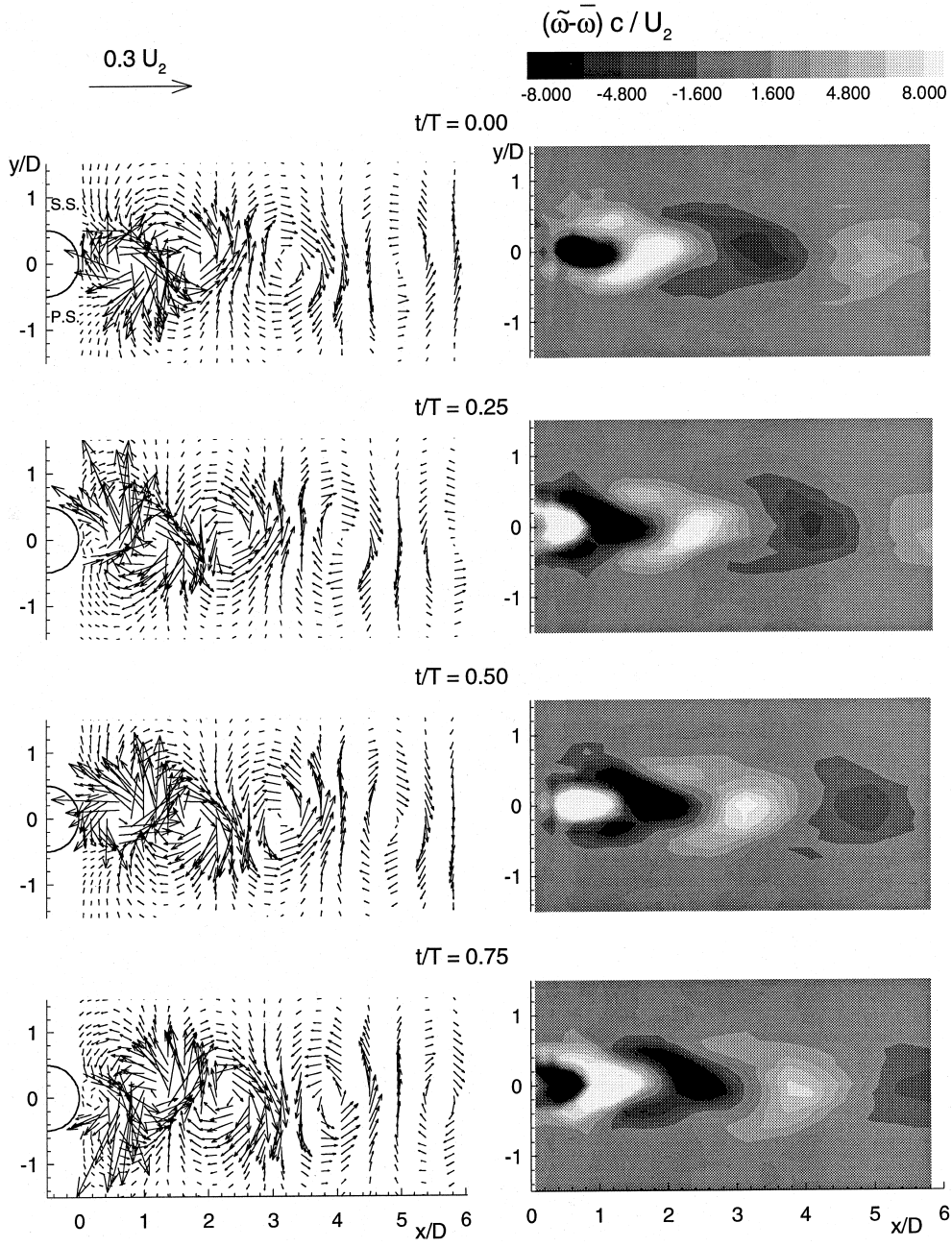

Fig. 6. Vector plots and vorticity contours of the periodic flow at successive phases.

The streamwise periodic velocity component $(\tilde{U}_s - \bar{U}_s)$ (left of Fig. 5) shows an anti-symmetric periodic structure with peaks and valleys which alternate on the pressure and the suction side of the wake proceeding in streamwise direction. The cross-stream periodic component $(\tilde{U}_n - \bar{U}_n)$ (right of Fig. 5) is structured in cores of positive and negative values, approximately centred in the wake, which alternate along the wake centreline. The nuclei of $(\tilde{U}_n - \bar{U}_n)$ appear displaced in respect of those of $(\tilde{U}_s - \bar{U}_s)$ of about half wavelength in streamwise direction.

The kinematic structure of the periodic flow, as comes out from the present results, looks qualitatively similar to that presented by Cantwell and Coles [2] for the wake downstream of a cylinder, but the magnitude of the periodic velocity components, made non-dimensional with the cascade outlet velocity U_2, is much lower. This difference may be attributed to various factors, like a less-defined vortex shedding frequency, the boundary layer state at separation, the ratio of the boundary layer thickness to the distance between the separation points and the flow acceleration in the cascade.

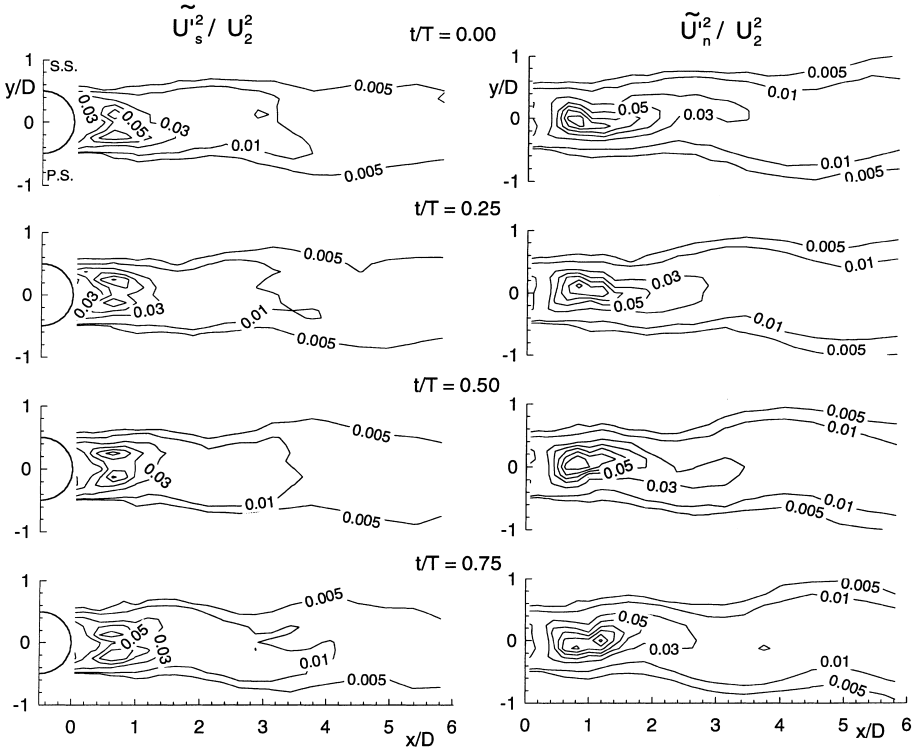

Fig. 7. Contours of the normal Reynolds stresses at successive phases.

The combination of the two velocity patterns $(\tilde{U}_s - \bar{U}_s)$ and $(\tilde{U}_n - \bar{U}_n)$ gives rise to the rolling up of the periodic flow in a row of vortices as shown by the vector plots of Fig. 6.

Vortices of opposite circulation are shed alternatively from both the trailing edge sides. The magnitude of the periodic velocity vectors attains values as large as 15–20% of the cascade outlet velocity U_2 in the near wake region with $x/D < 3$. Due to their periodic advection action, such large vortices are expected to play a significant role in the mixing out process of the near wake. From $x/D = 3$ onwards the magnitude of the velocity vectors is strongly reduced indicating a surprisingly fast dissipation of the kinetic energy of the periodic motion within few trailing edge diameters.

3.3. Vorticity

Identification of coherent structures and analysis of their evolution in time have been carried out with the aid of the periodic flow vorticity $(\tilde{\omega} - \bar{\omega})$. In Fig. 6, the vortices are highlighted by zones of positive and negative intense vorticity alternating in streamwise direction. The vorticity patterns are structured into individual nuclei of opposite vorticity located on opposite sides. The vortex centres lie very close to the wake centreline, in agreement with the findings of Cantwell and Coles investigation [2]. These nuclei extend backward by means of ribs embracing on the two sides the incoming nucleus of opposite vorticity. The ribs on the two sides of each vortex are characterised by a different level of vorticity with larger values on the side from which the vortex has been shed off. Local peaks of vorticity in the region $x/D \leqslant 3$ are very high. The peak values for the quantity $(\tilde{\omega} - \bar{\omega})\, c/U_2$ are of the order of 20, indicating that the local periodic vorticity is as large as 20 times the mean streamwise acceleration (U_2/c) that the flow undergoes through the cascade.

Concerning the mechanism of vortex shedding, two different modes are recognised [17]: a low speed mode and a high speed mode. The low speed mode described by Kovasznay [18] applies for cylinders with $Re_D < 400$. In this mode, the eddy street starts as trail instability and the eddies grow along the wake, while carried downstream. The high speed mode presents two distinct stages: formation and shedding. The eddies are formed behind the cylinder by the rolling up of the free-shear layer at a fixed location, and the eddy growth ceases when the feeding shear layer is cut off. This hypothesis is put forward by Gerrard [19], who postulates that at the end of the formation process of one vortex, fluid from the opposite side bearing vorticity of opposite sign is drawn across the axis. When this vorticity equals and cancels out the local vorticity, the vortex is shed off.

Gerrard's high speed eddy shedding model is helpful for interpreting the instantaneous pictures of the unsteady flow in the vortex formation region. In Fig. 6, the vortices shed from the suction side are clockwise and the associated vorticity is negative (black). At $t/T = 0.25$ (second frames from the top), a clockwise vortex extending from $x/D = 0$ on the suction side to $x/D = 1.7$ on the centreline, characterised by negative vorticity, is

shown just at the shedding instant. Fluid entrained from the pressure side is rolling up in a counterclockwise loop filling the base region. The positive (white) vorticity of this fluid tends to cancel out the local negative vorticity on the suction side at $x/D = 0.0$, causing the clockwise suction side vortex shedding.

At $t/T = 0.50$ (third frames), the clockwise suction side vortex has been shed off, while the core of positive vorticity associated with the pressure side vortex in formation is growing, being fed by the flow from the pressure side.

At $t/T = 0.75$ (fourth frames), half period after the suction side vortex shedding ($t/T = 0.25$), the periodic flow is in opposition of phase, the counterclockwise pressure side vortex, just before the shedding instant, possesses the maximum of positive vorticity. Negative vorticity is now entering in the base region from the suction side and the clockwise suction side vortex begins to form.

3.4. Reynolds stresses

The evaluation of Reynolds stress components due only to random fluctuations is made possible by the decomposition technique, which allows separating the random fluctuations from the periodic part of the signal. Fig. 7 shows the normal Reynolds stresses at four successive phases in a period ($t/T = 0, 0.25, 0.50, 0.75$). Streamwise and cross-stream normal Reynolds stresses are large in the wake region, with maxima of turbulence intensity larger than 25% and 30%, respectively. These values are comparable, but slighly lower than those found by Cantwell and Coles [2] in the wake of a circular cylinder. Different patterns for the two components, with a double-peak structure for the streamwise normal component and a single-maximum centred in the wake for the cross-stream normal component, result in large turbulence local anisotropy. A feature of the turbulent stress pattern is the low turbulence intensity of both components in a narrow zone in proximity of the trailing edge surface.

A certain degree of periodicity interests the turbulence quantities, as shown by the periodic change of curvature of the normal stress contours. Local contour line curvatures depend on the convective transport of the contra-rotating vortices, as can be inferred by comparing the contours of Fig. 7 with the vector plots of Fig. 6. Superposing the distribution of the cross-stream normal stress $\widetilde{U_n'^2}$ (Fig. 7, right side) and the vorticity distribution of Fig. 6 right side, it can be verified that the isocontours of relatively large values of normal stress correspond with the cores of periodic vorticity.

Considering the momentum equations for the phase-averaged flow [2], only the Reynolds stress terms due to random fluctuations appear, since the large-scale motion is accounted in the non-steady term. On the contrary, if global (time-averaged) equations are considered, additional terms due to the correlation of the large-scale periodic fluctuations have to be evaluated and introduced into the momentum balance [2]. Fig. 8 shows the

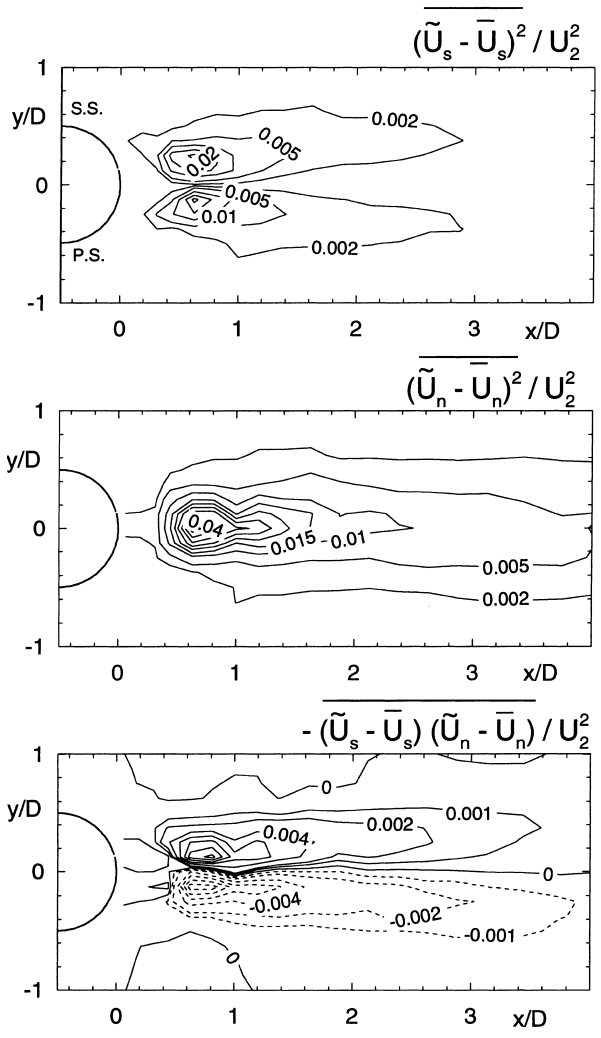

Fig. 8. Time-averaged stresses due to the periodic velocity fluctuations.

distributions of these terms obtained from the experimental data.

The normal components $\overline{(\tilde{U}_s - \bar{U}_s)^2}$ and $\overline{(\tilde{U}_n - \bar{U}_n)^2}$ reflect the distribution of the corresponding velocity fluctuations with a couple of peaks of different magnitude on the two sides of the wake for the streamwise component and a centred core of larger values for the cross-stream component. The normal stresses due to the periodic motion are appreciably lower, but of the same order of magnitude of the turbulent stresses. The rate of decay in streamwise direction is more rapid for the stresses associated with the periodic motion, because the mechanisms of production and dissipation are different for the two types of stresses. After the vortices are formed with accumulation of opposite vorticity from the two shear layers, the kinetic energy of the organised structures is dissipated by the deformation work [20] performed by the turbulent stresses on the strain field associated with the periodic motion and this dissipation is not compensated by production mechanisms. On the

other hand, the deformation work, appearing as a production term in the turbulence kinetic energy equation, acts to transfer energy from the large structures to the random turbulence fluctuations. As a consequence, viscous dissipation is partially balanced by production and the turbulent stresses decay at a slower rate.

The shear stress $-\overline{(U_s \simeq \bar{U}_s)(U_n \simeq \bar{U}_n)}$ associated with the large-scale periodic motion exhibits characteristic anti-symmetry with change of sign through the wake centreline. This shear stress, in accordance with that due to random fluctuations $-\widetilde{U_s' U_n'}$ acts to accelerate the flow in the wake central region decelerating the wake periphery. The von Karman vortex pattern is such that the periodic cross-stream velocities convey positive periodic streamwise momentum from the free-stream towards the interior of the wake.

4. Practical significance/usefulness

The results of the present work show that the wakes of turbine blades, similar to those of cylinders, are affected by von Karman vortex shedding. In the present experiment carried out at operating conditions representative of real gas turbines, the Strouhal number associated with the shedding frequency is higher than that of circular cylinders. Knowledge of the shedding frequency during the blade design phase is important in order to prevent blade resonance operating conditions.

Moreover, the present experiment provides details of the physics of the vortex shedding phenomenon from turbomachinery blades, which contribute to improve its understanding. The results constitute a comprehensive database suitable for validation of unsteady codes to be used for turbomachinery numerical simulations.

5. Conclusions

Time-varying properties of the flow in the near wake of a large-scale turbine blade have been experimentally investigated in detail by means of a two-component LDV and analysed by using a phase-locked ensemble averaging technique allowing the decomposition of the flow into mean, periodic and random contributions.

Due to the turbulent state of the boundary layers at the separation points, the time-mean recirculating flow zone at the trailing edge is appreciably shorter compared with the ones found in previous investigations on circular cylinders in the "shear layer transition regime". The rather high value for the Strouhal number ($St = 0.26$) of the present experiment, typical of cylinders with larger value of $Re_D (>10^6)$, is consistent with the short separation bubble found behind the blade trailing edge. The structure of the periodic flow is qualitatively in agreement with that described by Cantwell and Coles in the near wake of a cylinder at $Re_D = 140,000$, but the amplitudes of the periodic fluctuations in the present case are weaker.

Reconstruction of the time evolution of the periodic vector field and the associated periodic vorticity reveals the existence of a regular vortex street with peaks of opposite vorticity located very close to the wake centreline. These results support entirely the model of vortex formation proposed by Gerrard.

The shear stress associated with the large-scale periodic motion produce a flux of positive streamwise momentum from the periphery toward the interior of the wake.

Normal Reynolds stresses associated with the random fluctuations are larger and decay more slowly in streamwise direction compared with the normal stresses associated with the large-scale periodic motion. However, in the near wake region the two contributions are comparable and, therefore, stresses due to periodic velocity fluctuations cannot be neglected in the time-averaged momentum balance.

Acknowledgements

This work was performed under the BRITE-EURAM Contract AER2-92-0048, endorsed by MTU Munich and SNECMA Paris. These supports are gratefully acknowledged.

References

[1] G. Cicatelli, C.H. Sieverding, A Review of the Research on Unsteady Turbine Blade Wake Characteristics, AGARD PEP 85th Symposium on Loss Mechanisms and Unsteady Flows in Turbomachines, Derby, 1995.
[2] B. Cantwell, D. Coles, An experimental study of entrainment and transport in the turbulent near wake of a circular cylinder, J. Fluid Mech. 136 (1983) 321–374.
[3] D.A. Lyn, S. Einav, W. Rodi, J.-H. Park, A laser Doppler velocimetry study of ensemble-averaged characteristics of the turbulent near wake of a square cylinder, J. Fluid Mech. 304 (1995) 285–319.
[4] G. Cicatelli, C.H. Sieverding, The Effect of Vortex Shedding on the Unsteady Pressure Distribution Around the Trailing Edge of a Turbine Blade, ASME Paper No. 96-GT-359, 1996.
[5] P. Zunino, M. Ubaldi, U. Campora, A. Ghiglione, An experimental investigation of the flow in the trailing edge region of a turbine cascade, in: Proceedings of the Second European Conference on Turbomachinery Fluid Dynamics and Thermodynamics, Antwerpen, March 1997.
[6] W.E. Carscallen, H.U. Fleige, J.P. Gostelow, Transonic Turbine Vane Wake Flows, ASME Paper No. 96-GT-419, 1996.
[7] W.C. Reynolds, A.K. Hussain, The mechanics of an organized wave in turbulent shear flow. Part 3. Theoretical models and comparisons with experiments, J. Fluid Mech. 54 (2) (1972) 263–288.
[8] A. Boutier, Accuracy of Laser Velocimetry, Lecture Series 1991-05, VKI, Brussels, 1991.
[9] T. Strazisar, Laser Anemometry in Compressors and Turbines, ASME Lecture on Fluid Dynamics of Turbomachinery, 1986.
[10] D. Modarress, H. Tan, A. Nakayama, Evaluation of signal processing techniques in laser anemometry, in: Proceedings of the

Fourth International Symposium on Application of Laser Anemometry to Fluid Dynamics, Lisbon, July 1988.

[11] C.H. Sieverding, H. Heinemann, The influence of boundary layer state on vortex shedding from flat plates and turbine cascades, ASME J. Turbomachinery 112 (1990) 181–187.

[12] M. Ubaldi, P. Zunino, U. Campora, A. Ghiglione, Detailed velocity and turbulence measurements of the profile boundary layer in a large scale turbine cascade, ASME Paper No. 96-GT-42, 1996.

[13] BRITE EURAM AER2-92-0048, Time varying flow characteristics behind flat plates and turbine cascades, Final Technical Report, 1996.

[14] A.A. McKillop, F. Durst, A laser anemometry study of separated flow behind a circular cylinder, in: Proceedings of the Second International Symposium on Application of Laser Anemometry to Fluid Dynamics, Lisbon, July 1984.

[15] C. Williamson, Vortex dynamics in the wake of a cylinder, in: S.I. Green (Ed.), Fluid Vortices, Kluwer Academic Publishers, Dordrecht, 1995, pp. 155–234.

[16] R.D. Blevins, Vortex-structure interaction, in: S.I. Green (Ed.), Fluid Vortices, Kluwer Academic Publishers, Dordrecht, 1995, pp. 533–574.

[17] M.M. Zdravkovich, Flow Around Circular Cylinders, Oxford University Press, Oxford, 1997.

[18] L.S.G. Kovasznay, Hot wire investigations of the wake behind cylinders at low Reynolds numbers, Proc. Roy. Soc. A 198 (1949) 174–190.

[19] J.H. Gerrard, The mechanics of the formation region of vortices behind bluff bodies, J. Fluid Mech. 25 (2) (1966) 401–413.

[20] H. Tennekes, J.L. Lumley, A First Course in Turbulence, MIT Press, Cambridge, MA, 1978.